Gd_5Si_4 micro- and nano-particles for self-regulated magnetic hyperthermia

Z. Boekelheide[1] Z. A. Hussein[2] S. M. Harstad[3] A. A. El-Gendy[3,4,5] R. L. Hadimani[3]
[1]Department of Physics, Lafayette College, Easton PA 18042, USA
[2]Department of Electrical and Computer Engineering, Lafayette College, Easton PA 18042, USA
[3]Department of Mechanical and Nuclear Engineering, Virginia Commonwealth University, Richmond VA 23284, USA
[4]Nanotechnology and Nanometrology Laboratory, National Institute for Standards, Giza 12211, Egypt
[5]Department of Physics, University of Texas at El Paso, El Paso, TX 79968, USA

Gd_5Si_4 is a promising candidate for magnetic hyperthermia because its T_C is near the therapeutic range and is tuneable, opening the door for self-regulated hyperthermia which is limited from overheating by T_C. In addition, Gd_5Si_4 has a high saturation magnetization and is potentially biocompatible. In this paper, Gd_5Si_4 particles were fabricated by a scalable top-down approach of arc-melting and ball-milling. The particles have an average size of 900 nm and a wide size range. Magnetization measurements show that the magnetic transition is broadened and the transition temperature T_C is somewhat reduced from the bulk value of 63 °C to 50 °C, which is very close to the maximum desired hyperthermia temperature range of 43-45 °C. Hyperthermia measurements were performed in an alternating magnetic field. Specific loss power was calculated from the slope of the heating curve; the maximum value was 18 W/g at 0.064 T and 213 kHz. Self-regulated heating behavior was demonstrated, with maximum temperatures approaching 47 °C for the largest fields, close to the measured magnetic transition temperature T_C.

I. Introduction

One developing application of nanomedicine is magnetic hyperthermia cancer treatment. Magnetic hyperthermia, first proposed in 1957 [1], has been successful in clinical trials and is now available to some patients in Germany for treatment of glioblastoma, prostate cancer, and other cancers [2]. In magnetic hyperthermia treatment, magnetic particles are directed toward a cancerous tumor and an alternating magnetic field (AMF) is applied, with frequencies in the hundreds of kHz in the therapeutic range. This causes rapid switching of the particles' magnetic moments which results in heat dissipated equal to the area enclosed in the magnetic hysteresis loop $M(H)$ during each field cycle [3]. This heat can damage or kill cells of the tumor without damage to the normal cells, and can enhance other therapies such as radiation by preventing DNA-damage repair [4]. An important metric for the heat output of a particular material is the specific loss power (SLP), the power dissipated per gram of material, which is intimately related to the magnetic properties.

Currently, iron oxide nanoparticles are used in magnetic hyperthermia because of their high SLP and their biocompatibility [5]. However, there could be benefits to using other materials. One potentially beneficial magnetic property is a Curie temperature T_C around the desired treatment temperature (43-45 °C) so that the heating is self-regulating, preventing accidental overheating of healthy cells. Several candidate materials have been proposed for self-regulated hyperthermia, typically compounds or alloys in which the stoichiometry can be varied to tune the Curie temperature [6], [7]. One candidate material for self-regulated hyperthermia is Gd_5Si_4 and related alloys [8]. Bulk Gd_5Si_4 has a high magnetization with $T_C = 63°$ C [9]. Gd_5Si_4 micro- and nano-particles have a decreased T_C which makes this material even more promising [10].

Although full cytotoxicity studies have not yet been done, Gd_5Si_4 particles are potentially biocompatible. Free Gd^{3+} ions are toxic, but chelated Gd salts are biocompatible and FDA-approved for use as MRI contrast agents [11], [12]. In addition, coated Gd_2O_3 nanoparticles have been shown to be nontoxic and are also candidates for contrast agents [13]. Silicon is biocompatible and Si and Si-based materials are used as coatings for biomedical implants [14], [15]. The high stability of Gd_5Si_4 is promising for biocompatibility.

The combination of high magnetization, potential for biocompatibility, and the potential for self-regulated hyperthermia makes these particles an exciting direction for exploration.

II. Experimental Methods

Gd_5Si_4 particles were synthesized using arc-melting of the stoichiometric mixture of Gd (purity 99.9 %) and Si (Cerac Inc., USA, >99.999%) under Ar atmosphere. The arc-melting process was repeated six times to ensure homogeneity. To obtain sub-micron Gd_5Si_4 particles, the as-cast material was first ground in an agate mortar and screened to obtain powders with particle size of 50 μm or smaller. Further reduction in the particle size was achieved by high-energy ball-milling of the powder in a SPEX 8000M mill. All millings and subsequent manipulations were performed in a glove box in an argon atmosphere. In the milling procedure, powder to ball weight ratio of ∼5:1 was used with 2 balls of 11 mm diameter and 4 balls of 4 mm diameter. 10% by weight poly(ethylene glycol) (PEG) (molecular weight-8000 Da) was added to the Gd_5Si_4 powder to act as a surface modifier during milling. A two-step milling process was used in which the powder and PEG mixture was initially milled for 1 h at which point the milling

Corresponding author: Zoe Boekelheide (boekelhz@lafayette.edu)

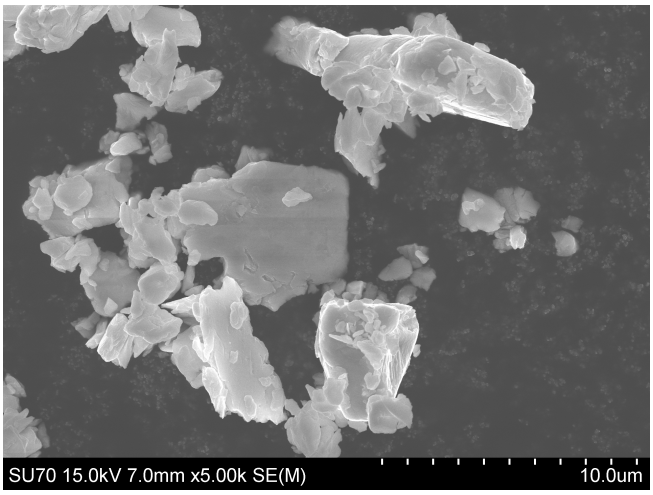

Fig. 1. Scanning Electron Microscopy (SEM) image showing micro- (foreground) and nano- (background) particles of Gd_5Si_4.

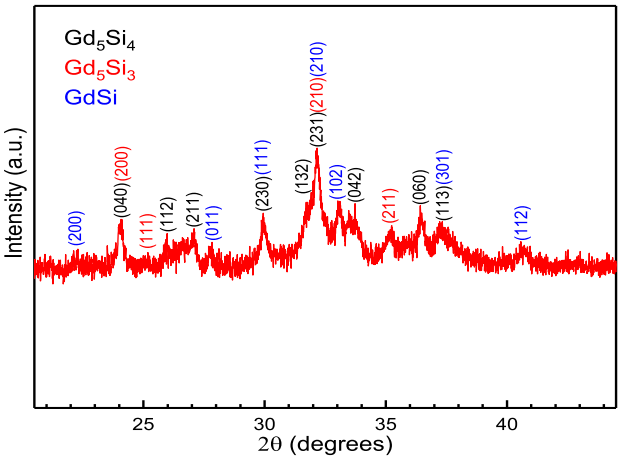

Fig. 2. X-ray diffraction of particles showing the positions of characteristic peaks for Gd_5Si_4 as well as the main impurity phases Gd_5Si_3 and GdSi.

was interrupted and 5 ml of heptane was added to reduce binding of the particles due to localized melting and retain crystallinity [10]. The milling was then continued for another 1 h. After milling, the heptane was evaporated to yield fine Gd_5Si_4 powder mixed with PEG.

The Gd_5Si_4 particles were analyzed for morphology and size using scanning electron microscopy (SEM, Hitachi Model SU-70). X-ray diffraction (XRD, PANalytical MPD XPert Pro) was collected using a Cu Kα X-ray source. A vibrating sample magnetometer (VSM, Quantum Design, 3T Versalab) was used to investigate the magnetic properties of the particles.

For magnetic hyperthermia measurements, an Ambrell EasyHeat AMF generator was used with a homebuilt solenoidal coil operating at frequencies between 213-217 kHz. The eight-turn solenoidal coil is water-cooled and has been described elsewhere [16]. The field strength inside the coil has been calibrated with a Fluxtrol alternating magnetic field probe. The peak field amplitude is not exactly the same for each field cycle, so the parameter $\mu_0 H_{max}$ is given in terms of the root mean square (rms) field strength: $\mu_0 H_{max} = \sqrt{2}\mu_0 H_{rms}$. A fiber-optic sensor (Opsens OTG-M170) recorded the temperature of the sample versus the time ($T(t)$) as current was applied to the solenoid.

The specific loss power (SLP) was measured calorimetrically by placing a sample of 0.0326 g of particles + PEG dispersed in 500 μL of H_2O in a flat-bottomed glass vial. With a starting temperature of about 22.0 °C, the AMF was applied for a short time interval in order to achieve a temperature change ΔT of about 1 °C, then the AMF was removed and the sample was allowed to cool to 22.0 °C. The process was repeated for a range of AMF amplitudes. SLP was calculated from the slope of the temperature rise upon application of the AMF:

$$SLP = \frac{cm_w}{m_p}\left(\frac{dT}{dt}\right) \quad (1)$$

where c is the specific heat capacity of water, m_w is the mass of water, and m_p is the mass of the particles. The heat capacity of the sample is assumed to be dominated by the water.

The validity of (1) to calculate the SLP relies on temperature uniformity within the volume of the sample. Although slight sedimentation of the larger particles in this sample was observed, in the flat-bottomed container the sediment spread evenly over the bottom of the container and the temperature of the sample was found to be approximately uniform throughout its volume, as determined by placing the fiber-optic temperature sensor at different locations within the sample. Thus, the SLP calculation by (1) is valid for this measurement.

Testing the self-regulating hyperthermia potential of the particles required different experimental parameters in order to explore the highest temperatures. We used the same sample of particles + PEG, in a smaller volume of H_2O (250 μL), in a plastic container with a conical bottom. In a container with a conical bottom, the sedimentation leads to a high concentration of particles near the nadir of the container. We placed the fiber optic temperature sensor near this bottom point and measured the temperature as the field was turned on and allowed to stabilize to a steady-state maximum temperature. In this case, the temperature is highest at this bottom point compared to other points in the suspension.

III. Results

A. Sample characterization

Figure 1 shows an SEM image of the particles. The morphology of the formed particles shows random shape and a wide size range with an average particle size of 900 nm. X-ray diffraction, shown in Figure 2, provides details on the crystal structure of the particles. Preparation of Gd_5Si_4 using commercial purity gadolinium leads to the formation of a small amount of Gd_5Si_3 and GdSi impurities in the predominantly Gd_5Si_4 matrix. Gd_5Si_3 can be identified by the peak around 35° while the peaks at around 22° and 41° indicate the presence of GdSi phase.

The magnetization as a function of temperature (Fig. 3) shows that the Gd_5Si_4 particles are ferromagnetic up to around 50 °C. However, the transition is broad, with a peak in

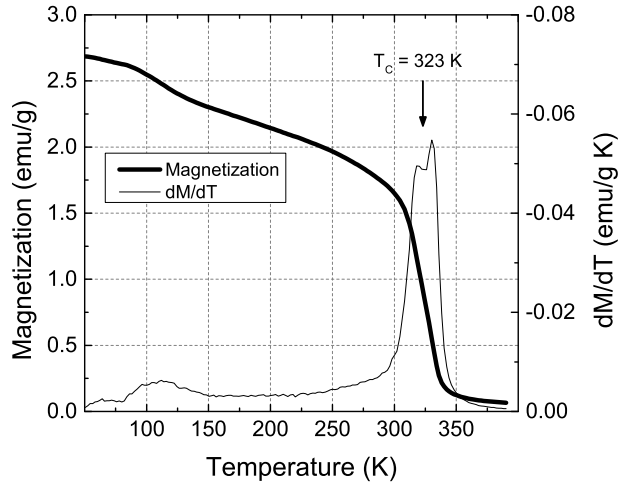

Fig. 3. Magnetization (M) (thick line) and dM/dt (thin line) as a function of temperature (T) at a magnetic field of 0.01 T.

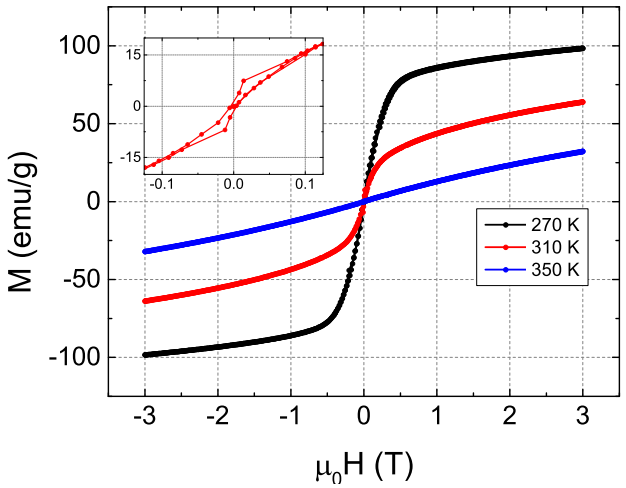

Fig. 4. Magnetic hysteresis loops at temperatures of 270 K, 310 K, and 350 K. Inset: 310 K data at low fields.

dM/dT about 28 °C in width. This T_C is reduced from the bulk value of 63 °C, putting it close to the therapeutic temperature range for magnetic hyperthermia. Both GdSi and Gd_5Si_3 order antiferromagnetically, with T_N reported as 50 K and 55 K, respectively [17], [18]. Thus, both main impurity phases have a very small influence on magnetic properties at room temperature.

$M(H)$ at 270 K, 310 K, and 350 K is shown in Figure 4, indicating ferromagnetic behavior at 270 K and 310 K, below T_C, and paramagnetic behavior at 350 K, above T_C. The figure inset shows a close up of the 310 K data, showing hysteresis behavior.

B. Magnetic hyperthermia results

1) Specific loss power

The temperature as a function of time for several AMF cycles for the SLP measurements, described in Section II, is shown in Figure 5(a). The SLP, calculated from the slope of $T(t)$, is shown in Figure 5(b). The magnitude of the SLP is on the low end of the very wide range of reported SLP values in the literature, which consists of mostly iron oxide particles [3]. The SLP as a function of field increases rapidly between 0.01-0.03 T, after which it increases more slowly. Theoretically, the SLP is expected to increase as H_{max}^2 at low fields, for both nanoparticles and macroscopic particles [6], [19]; the red curve shows a fit to H_{max}^2 of the data from $\mu_0 H_{max} = 0 - 0.03$ T. The H_{max}^2 behavior comes from an assumption of a linear relationship between M and H, which may be a good approximation at low fields, but often is not valid at higher fields. While $M(H)$ during approximately a microsecond-long AMF cycle may differ from the quasistatic $M(H)$ shown in Figure 4, the hysteresis loop shown in Figure 4 strongly suggests that nonlinear behavior of $M(H)$ should be expected for fields above 0.03 T. This plateau in SLP has been previously reported by other researchers at large field strengths [20], [21].

The "biological discomfort level" put forth by Hergt [22] for tolerance of an AMF during hyperthermia treatment of small areas of the body and serious illness is $H_{max} f = 5 \times 10^9$ A m^{-1} s^{-1}, which for a frequency of 213 kHz translates to a maximum field of 0.028 T in the therapeutic range. The maximum therapeutic field occurs around the beginning of the plateau in SLP, so that at the maximum therapeutic field, the SLP is close to maximum. This is promising for potential therapeutic use.

2) Self-regulation of hyperthermia

A sample steady-state heating curve showing the maximum temperature reached is shown in Figure 6(a), for a field of 0.064 T. Here, the temperature reaches a maximum of 45.3 °C before the field is turned off. Similar heating curves were acquired for various field amplitudes. The maximum temperature achieved by such measurements as a function of field is shown in Figure 6(b).

The maximum temperature achieved in the largest fields approaches 47 °C as the field is increased, close to the measured T_C for these Gd_5Si_4 particle samples. The magnetic transition is broad, so the magnetization decreases significantly in the temperature range between 37 and 65 °C. As the magnetization decreases, the heating should decrease, so it will become increasingly difficult to heat the sample as the temperature increases into the magnetic transition region. Thus, hyperthermia in these samples is self-regulating, in these measurements never achieving a temperature above $T_C = 47$°C.

IV. Discussion

The polydisperse Gd_5Si_4 micro- and nano-particles fabricated for this study show a broadened magnetic transition with T_C decreased from the bulk value of 63 °C to 50 °C. This is likely tuneable based on the preparation conditions (milling time and particle size) [10]. Explanations for the changes in magnetic transition temperature are still under investigation, however they may arise from effects of disorder and/or from microstrains in the ball-milled particles. The wide range of particle sizes in the sample described here likely indicates a distribution of properties throughout the sample and explains

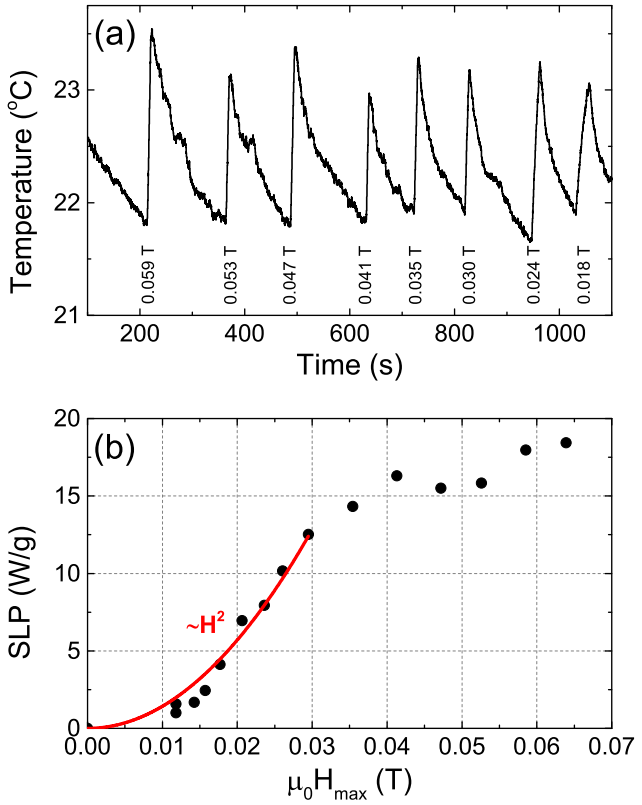

Fig. 5. (a) Heating curves of 0.0326 g of particles with PEG in 500 μL of H_2O in a flat-bottomed container, used for SLP calculations. Each period of temperature increase corresponds to a different AMF amplitude. The frequency ranges from 213-217 kHz depending on AMF amplitude. (b) SLP calculated from the slope dT/dt in the temperature range 22.1-22.9 °C.

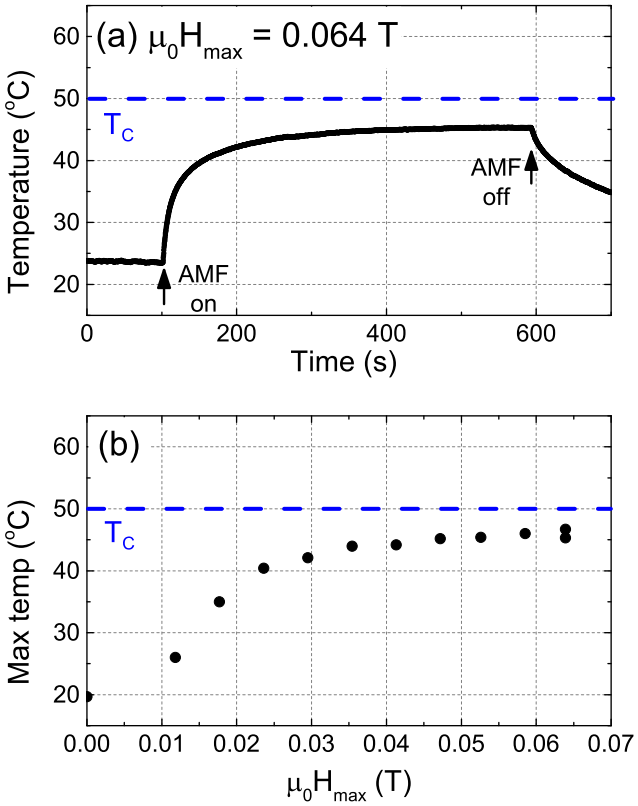

Fig. 6. (a) Heating curve for 0.0326 g of particles with PEG in 250 μL of H_2O in a container with a conical bottom, in an applied AMF with peak field amplitude of 0.064 T and frequency of 213 kHz. (b) Maximum temperature reached for this sample as a function of applied field amplitude, showing that the maximum temperature reached is 47 °C, close to the Curie temperature of the sample.

the broad magnetic transition. In order to better understand and to optimize the SLP and T_C of Gd_5Si_4 particles, it is important that future studies address this polydispersity by performing size selection on particle samples and thoroughly characterizing the size distributions. For the smallest particles, the relaxation time may approach the $\sim$ microsecond AMF cycle time (the superparamagnetic regime), which will change the character of the heat generation under an AMF for hyperthermia [23]. In this case, T_C would mark the transition from the superparamagnetic to the paramagnetic state, and heating would still be regulated by T_C.

V. Conclusion

Gd_5Si_4 particles prepared from a scalable top-down approach show promise for self-regulated magnetic hyperthermia. Future work will address size-selected particles, in particular the smaller nanoparticles, to understand the differences between larger and smaller nanoparticles and optimize the SLP and T_C.

Acknowledgment

Z. A. H. thanks the Bolton Fund for Research Experiences in Math, Biology, Physics, and Chemistry for support. Thanks to Shalabh Gupta and Vitalij K. Pecharsky, Ames Laboratory, U.S. Department of Energy, Office of Basic Energy Sciences, Division of Materials Science and Engineering through Iowa State University under Contract DE-AC02-07CH11358, for their assistance in preparing the nanoparticles. Thanks to the Nanomaterials Core Characterization Facility at Virginia Commonwealth University, for XRD, SEM, and VSM use. Thanks to Michael Karner at Lafayette College for making the solenoidal coil.

References

[1] R. K. Gilchrist, R. Medal, W. D. Shorey, R. C. Hanselman, J. C. Parrott, and C. B. Taylor, "Selective inductive heating of lymph nodes," *Ann. Surg.*, vol. 146, p. 597, 1957.

[2] Magforce, the nanomedicine company, `http://www.magforce.de/en/home.html`, Accessed Jan. 4, 2017.

[3] A. Hervault and N. T. K. Thanh, "Magnetic nanoparticle-based therapeutic agents for thermo-chemotherapy treatment of cancer," *Nanoscale*, vol. 6, p. 11553, 2014.

[4] J. L. R. Roti, "Cellular responses to hyperthermia (40-46°C): Cell killing and molecular events," *Int. J. of Hypertherm.*, vol. 24, p. 3, 2008.

[5] E. A. Perigo, G. Hemery, O. Sandre, D. Ortega, E. Garaio, F. Plazaola, and F. J. Teran, "Fundamentals and advances in magnetic hyperthermia," *Applied Physics Reviews*, vol. 2, p. 041302, 2015.

[6] A. H. El-Sayed, A. A. Aly, N. I. El-Sayed, M. M. Mekawy, and A. A. El-Gendy, "Calculation of heating power generated from ferromagnetic thermal seed (PdCo-PdNi-CuNi) alloys used as interstitial hyperthermia implants," *J. Mater. Sci.: Mater. Med.*, vol. 18, p. 523, 2007.

[7] K. S. Martirosyan, "Thermosensitive magnetic nanoparticles for self-controlled hyperthermia cancer treatment," *J. Nanomed. Nanotechnol.*, vol. 3, p. 1000e112, 2012.

[8] S. N. Ahmad and S. A. Shaheen, "Optimization of Gd_5Si_4 based materials: A step toward self-controlled hyperthermia applications," *J. Appl. Phys.*, vol. 106, p. 064701, 2009.

[9] F. Holtzberg, R. Gambino, and T. McGuire, "New ferromagnetic 5:4 compounds in the rare earth silicon and germanium systems," *Journal of Physics and Chemistry of Solids*, vol. 28, no. 11, p. 2283, 1967.

[10] R. L. Hadimani, S. Gupta, S. M. Harstad, V. K. Pecharsky, and D. C. Jiles, "Investigation of room temperature ferromagnetic nanoparticles of Gd_5Si_4," *IEEE Trans. Mag.*, vol. 51, p. 2504104, 2015.

[11] J. Endrikat, K. Vogtlaender, S. Dohanish, T. Balzer, and J. Breuer, "Safety of gadobutrol: Results from 42 clinical phase II to IV studies and postmarketing surveillance after 29 million applications," *Investigative Radiology*, vol. 51, p. 537, 2016.

[12] A. D. Sherry, P. Caravan, and R. E. Lenkinski, "A primer on gadolinium chemistry," *J. Magn. Reson. Imaging*, vol. 30, p. 1240, 2009.

[13] J. Y. Park, M. J. Baek, E. S. Choi, S. Woo, J. H. Kim, T. J. Kim, J. C. Jung, K. S. Chae, Y. Chang, and G. H. Lee, "Paramagnetic ultrasmall gadolinium oxide nanoparticles as advanced T_1 MRI contrast agent: Account for large longitudinal relaxivity optimal particle diameter, and in vivo T_1 MR images," *ACS Nano*.

[14] S. Z. Khalajabadi, M. R. A. Kadir, S. Izman, and M. Kasiri-Asgarani, "Microstructural characterization, biocorrosion evaluation and mechanical properties of nanostructured ZnO and Si/ZnO coated Mg/HA/TiO_2/MgO nanocomposites," *Surface and Coatings Technology*, vol. 277, p. 30, 2015.

[15] H. Bakhsheshi-Rad, E. Hamzah, M. Daroonparvar, M. Yajid, and M. Medraj, "Fabrication and corrosion behavior of Si/HA nano-composite coatings on biodegradable Mg-Zn-Mn-Ca alloy," *Surface and Coatings Technology*, vol. 258, p. 1090, 2014.

[16] Z. Boekelheide, Z. A. Hussein, and S. Hartzell, "Electronic measurements in an alternating magnetic field for studying magnetic nanoparticle hyperthermia: Minimizing eddy current heating," *IEEE Trans. Mag*, vol. 52, p. 5400304, 2016.

[17] E. V. Ganapathy, K. Kugimiya, H. Steinfink, and D. I. Tchernev, "Magnetic properties of some rare earth silicides: GdSi, Gd_5Si_3, $Dy_{5-x}Nd_x$ Si_3," *Journal of the Less-Common Metals*, vol. 44, p. 245, 1976.

[18] F. Canepa, S. Cirafici, and M. Napoletano, "Magnetic properties of Gd_5T_3 intermetallic compounds (T=Si,Ge,Sb)," *Journal of Alloys and Compounds*, vol. 335, p. L1, 2002.

[19] R. E. Rosensweig, "Heating magnetic fluid with alternating magnetic field," *J. Magn. Magn. Mater.*, vol. 252, p. 370, 2002.

[20] C. L. Dennis, K. L. Krycka, J. A. Borchers, R. D. Desautels, J. van Lierop, N. F. Huls, A. J. Jackson, C. Gruettner, and R. Ivkov, "Internal magnetic structure of nanoparticles dominates time-dependent relaxation processes in a magnetic field," *Advanced Functional Materials*, vol. 25, p. 4300, 2015.

[21] B. E. Kashevsky, S. B. Kashevsky, and I. V. Prkohorov, "Dynamic magnetic hysteresis in a liquid suspension of acicular maghemite particles," *Particuology*, vol. 7, p. 451, 2009.

[22] R. Hergt and S. Dutz, "Magnetic particle hyperthermia—biophysical limitations of a visionary tumour therapy," *Journal of Magnetism and Magnetic Materials*, vol. 31, p. 187, 2007.

[23] S. Ruta, R. Chantrell, and O. Hovorka, "Unified model of hyperthermia vis hysteresis heating in systems of interacting magnetic nanoparticles," *Scientific Reports*, vol. 5, p. 9090, 2015.